

Supporting Information

Facile Construction of Well-Defined Radical Metallacycles through Coordination-Driven Self-Assembly

Qian Tu,^a Gui-Fei Huo,^a Haitao Sun,^b Xueliang Shi^{*a} and Hai-Bo Yang^{*a}

^aShanghai Key Laboratory of Green Chemistry and Chemical Processes, School of Chemistry and Molecular Engineering, Chang-Kung Chuang Institute, East China Normal University 3663 N. Zhongshan Road, Shanghai 200062, P. R. China

^bState Key Laboratory of Precision Spectroscopy, School of Physics and Electronic Science, East China Normal University, Shanghai 200241, P. R. China

Contents

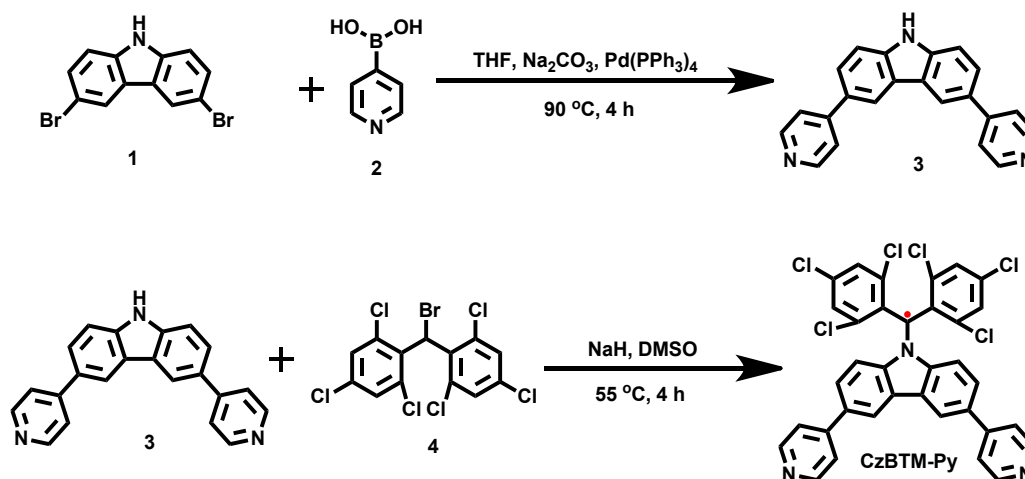
1 General.....	2
2 Synthesis and characterization.....	3
2.1 Synthesis of CzBTM-Py	3
2.2 Self-assembly of M1 and M2	4
2.3 Single crystal growth	5
3 EPR studies and additional EPR spectra.....	6
4 Single crystal data	11
5 NMR spectra of new compounds.....	14
6 Mass spectra of new compounds	18
7 Photophysical properties.....	19
8 Theoretical calculations results.....	21
9 Reference	22

1 General

All solvents were dried according to the standard procedures and all of them were degassed under N₂ for 30 minutes before use. All air-sensitive reactions were carried out under inert N₂ atmosphere. ¹H NMR, ¹³C NMR and ³¹P NMR spectra were recorded at 500 MHz with a Mercury plus 500 spectrometer at 298 K. The ¹H and ¹³C NMR chemical shifts are reported relative to the residual solvent signals and ³¹P NMR resonances are referenced to an internal standard sample of 85% H₃PO₄ (δ 0.0). Coupling constants (*J*) are denoted in Hz and chemical shifts (δ) are denoted in ppm. Multiplicities are denoted as follows: s = singlet and d = doublet. The HR-ESI mass spectra were performed on an Agilent (Santa Clara, CA, USA) ESI-TOF mass spectrometer (6224), acetonitrile as solvent. CW X-band EPR spectra for radicals were acquired on Bruker EMX instrument EMXPLUS-10/12. The single crystals were measured on Bruker Apex duo equipment with Cu radiation (λ = 1.54184 Å) at 100 K and the data sets were treated with the SQUEEZE program to remove highly disordered solvent molecules. Thermogravimetric analysis (TGA) were acquired on PerkinElmer STA 8000. UV-vis spectra were recorded in a quartz cell (light path 10 mm) on a Shimadzu UV2700 UV-visible spectrophotometer. Steady-state fluorescence spectra were recorded in a conventional quartz cell (light path 10 mm) on a Shimadzu RF-600 fluorescence spectrophotometer. Fluorescence lifetimes were recorded in a quartz cell (light path 10 mm) on the Edinburgh FLS980 transient fluorescence spectrometer. All spectral measurements were made at room temperature.

2 Synthesis and characterization

2.1 Synthesis of CzBTM-Py



Scheme S1. Synthetic route to compound CzBTM-Py.

Compound 3

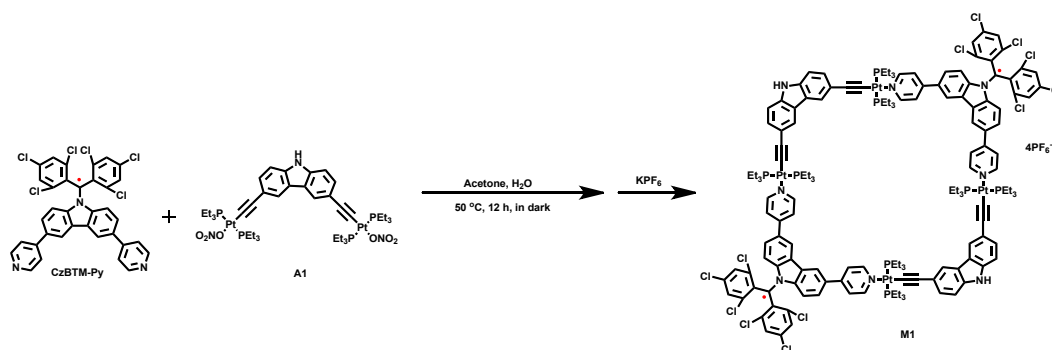
Synthesis of compound **3**. A degassed solution of the 3,6-dibromocarbazole (5.0 g, 15.0 mmol) in THF/H₂O (4:1, 200 mL) were added 4-pyridinylboronic acid (11.4 g, 90.0 mmol), Pd(PPh₃)₄ (1.8 g, 1.5 mmol) and Na₂CO₃ (6.5 g, 61.0 mmol). The resultant solution was stirred at 80 °C for 48 h under an inert atmosphere. The solvent was then removed by evaporation on a rotary evaporator. The residue was purified by column chromatography on silica gel (dichloromethane : acetone = 1 : 1, two drops of NEt₃) to get the **3** (2.4 g, 50% yield) as a pale-yellow solid. ¹H NMR (500 MHz, DMSO-*d*₆, ppm): δ 11.67 (s, 1H), 8.83 (s, 2H), 8.64 (d, *J* = 5.4 Hz, 4H), 7.91 (d, *J* = 8.5 Hz, 2H), 7.85 (d, *J* = 5.5 Hz, 4H), 7.64 (d, *J* = 8.5 Hz, 2H), ¹³C NMR (126 MHz, DMSO-*d*₆) δ 150.23 , 147.95, 141.01, 127.97, 124.93, 123.46, 121.01, 119.39, 111.99. HR-EI-MS: *m/z* calculated for C₂₂H₁₅N₃ [M]⁺: 321.1266, found: 321.1270.

Compound CzBTM-Py

Synthesis of compound CzBTM-Py. Under N₂ atmosphere, sodium hydride (60% in oil, 58.7 mg, 1.5 mmol) was dispersed in a solution of anhydrous dimethyl sulfoxide (20 mL), **3** (500.0 mg, 1.6 mmol) dissolved in anhydrous dimethyl sulfoxide (5 mL) was added dropwise and stirred until that no gas was generated. **4**^[1] (458.3 mg, 1.0 mmol) was added into the mixture and stirred for 3 h under

55 °C. Next, the mixture was cooled to room temperature and saturated ammonium chloride solution (50 mL) was added slowly. The precipitate was collected by suction filtration and purified by flash column chromatography (silica gel, dichloromethane : petroleum ether = 1 : 8), after that, PTLC was carried out to get the pure product **CzBTM-Py** (150.0 mg, 24% yield). HR-ESI-MS: m/z calculated for $C_{35}H_{18}Cl_6N_3$ $[M + H]^+$: 692.9602, found: 692.9672.

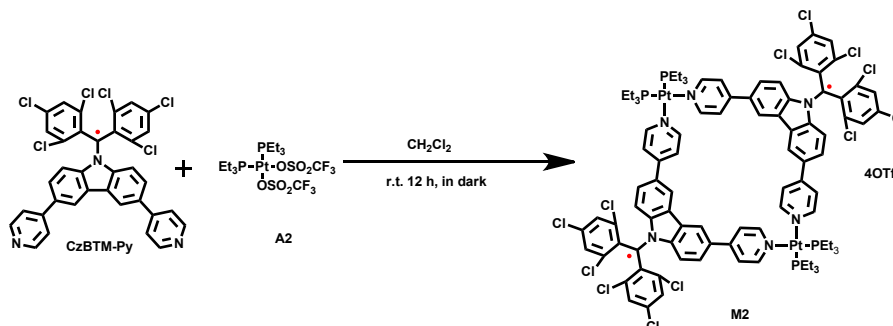
2.2 Self-assembly of M1 and M2



Scheme S2. Synthetic route to metallacycle **M1**.

Synthesis of metallacycle M1

Self-assembly of metallacycle **M1**. **CzBTM-Py** (20.0 mg, 28.8 μmol) and the organoplatinum 90° acceptor **A1**^[2] (34.6 mg, 28.8 μmol) were weighed accurately into a glass vial, and then added 5.0 mL acetone and 1.0 mL water. The reaction solution was then stirred at 55 °C in dark overnight to yield a homogeneous fuchsia solution. Then the saturated KPF_6 was added into the bottle with continuous stirring (5 min) to precipitate the product. The reaction mixture was centrifuged, washed several times with water, and dried by freeze-dryer. The product **M1** was obtained in 90% (53.4 mg) yield.



Scheme S3. Synthetic route to metallacycles **M2**.

Synthesis of metallacycle **M2**

Self-assembly of metallacycle **M2**. **CzBTM-Py** (10.0 mg, 14.4 μmol) and the organoplatinum 90° acceptor **A2**^[3] (10.5 mg, 14.4 μmol) were weighed accurately into a glass vial, and then added 2.0 mL CH_2Cl_2 , the reaction solution was then stirred at room temperature in the dark for 12 hours. After removing most of solvents, some drops of ether was added to precipitate the products, and the reaction mixture was centrifuged, washed several times with ether. Fuchsia powder **M2** was gained in 90% (18.4 mg) yield after drying the residue.

2.3 Single crystal growth

Single crystal of **CzBTM-Py**

CzBTM-Py was grown via a vapor diffusion method: ligand **CzBTM-Py** (1.0 μmol) was dissolved in chloroform (0.5 mL) solution and placed it in a 4.0 mL bottle. The small bottle was then placed in a 20.0 mL glass bottle containing methanol (1 mL) for 2 weeks, after that the dark red crystal **CzBTM-Py** was obtained.

Single crystal of **M1**

M1 was grown via a vapor diffusion method: metallacycles **M1** (1.0 μmol) was dissolved in dichloromethane (0.5 mL) solution and placed it in a 4.0 mL bottle. The small bottle was then placed in a 20.0 mL glass bottle containing isopropyl ether (1 mL) for 2 weeks, after that the dark red crystal **M1** was obtained.

Single crystal of **M2**

M2 was grown via a vapor diffusion method: metallacycle **M2** (1.0 μmol) was dissolved in dichloromethane (0.5 mL) solution and placed it in a 4.0 mL bottle. The small bottle was then placed in a 20.0 mL glass bottle containing isopropyl ether (1.0 mL) for a month, after that the dark red crystal **M2** was obtained.

3 EPR studies and additional EPR spectra

CW X-band EPR spectra for radicals were acquired on Bruker EMX instrument EMXPLUS-10/12. The samples were typically contained in 4.0 mm EPR sample tubes. The liquid sample was encapsulated in a 0.9 mm × 80.0 mm capillary tube and then placed in a special EPR sample tube. The solid samples were placed directly in the EPR sample tube for testing. The concentration of free radical remained consistent (10^{-3} mol L⁻¹) in all the testing liquid samples. The EPR intensity of the solution of **CzBTM-Py**, **M1** and **M2** was measured over 1000 min in the dark condition. The EPR intensity of the solution of **CzBTM-Py**, **M1** and **M2** was also measured under irradiation (LOT- QuantumDesign GmbH).

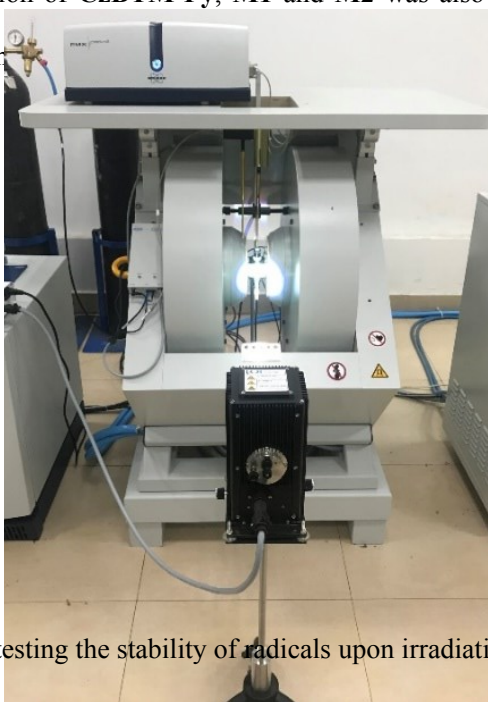


Figure S1. Instrument for testing the stability of radicals upon irradiation at 298 K.

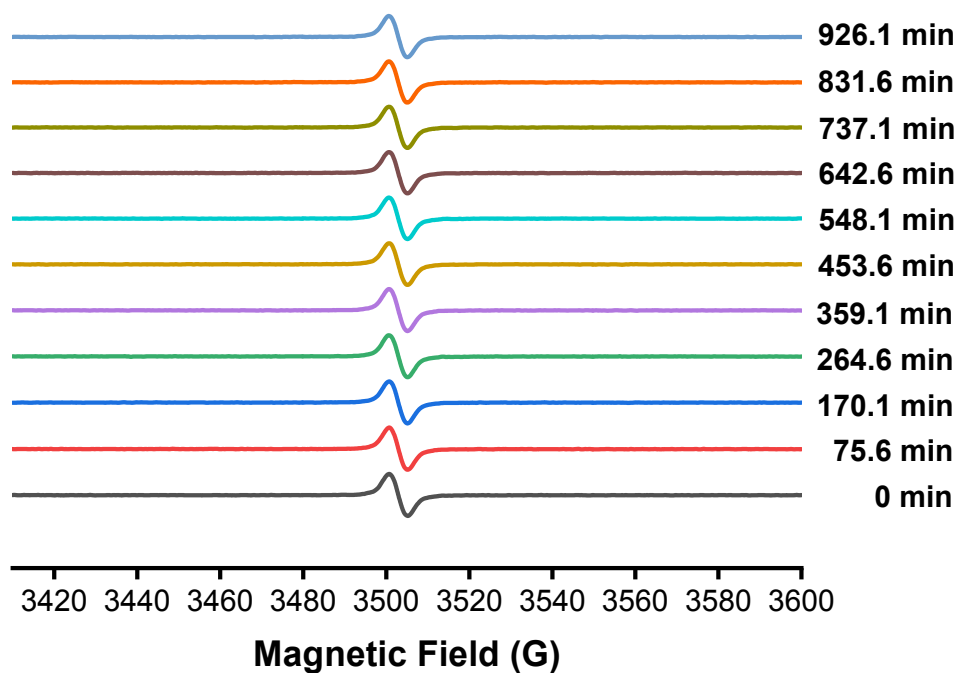


Figure S2. EPR signal fading of CzBTM-Py (1 mM in N, N-dimethylformamide) in the dark condition at 298 K.

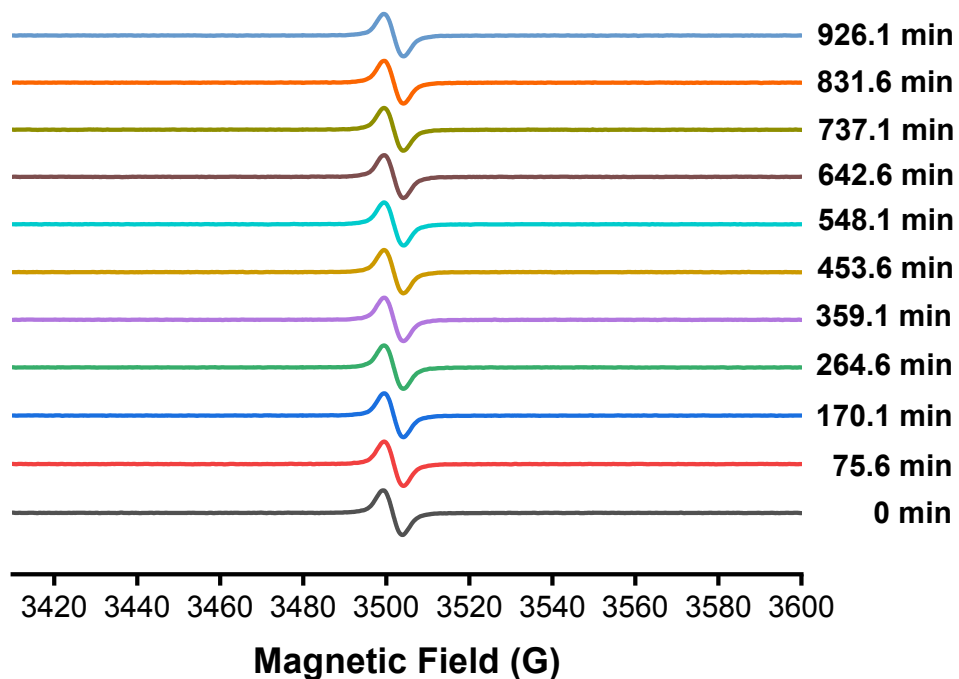


Figure S3. EPR signal fading of M1 (1 mM in N, N-dimethylformamide) in the dark condition at

298 K.

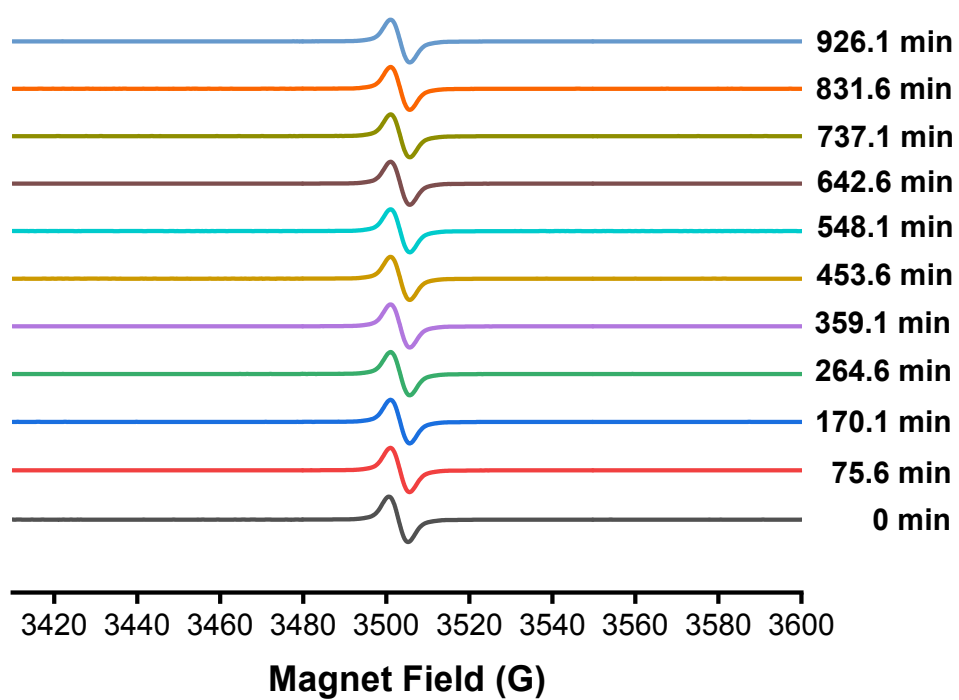


Figure S4. EPR signal fading of **M2** (1 mM in N, N-dimethylformamide) in the dark condition at 298 K.

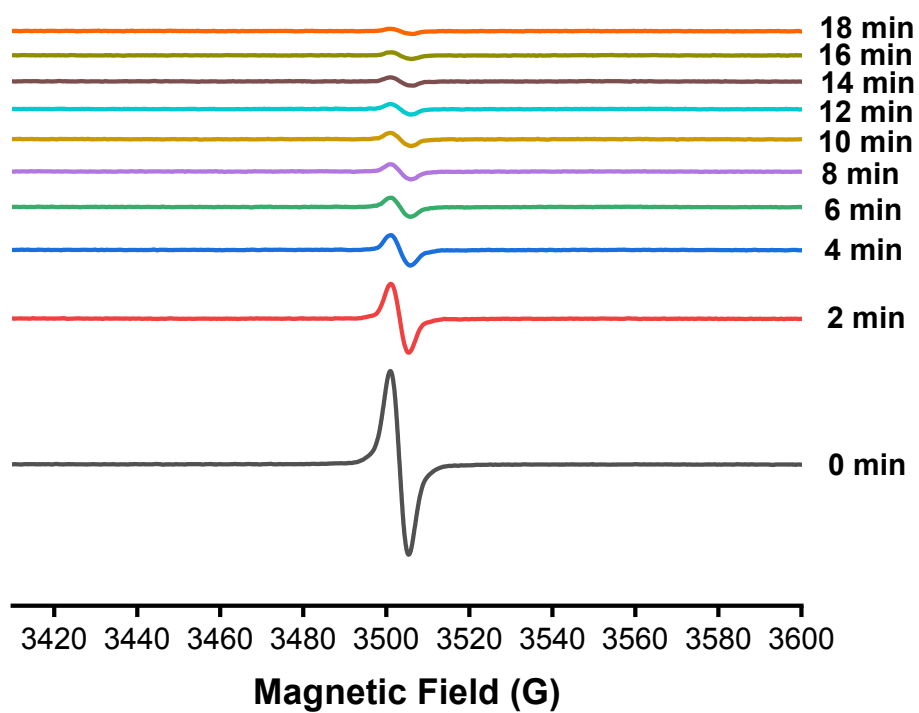


Figure S5. EPR signal fading of CzBTM-Py (1 mM in N,N-dimethylformamide) upon irradiation at 298 K.

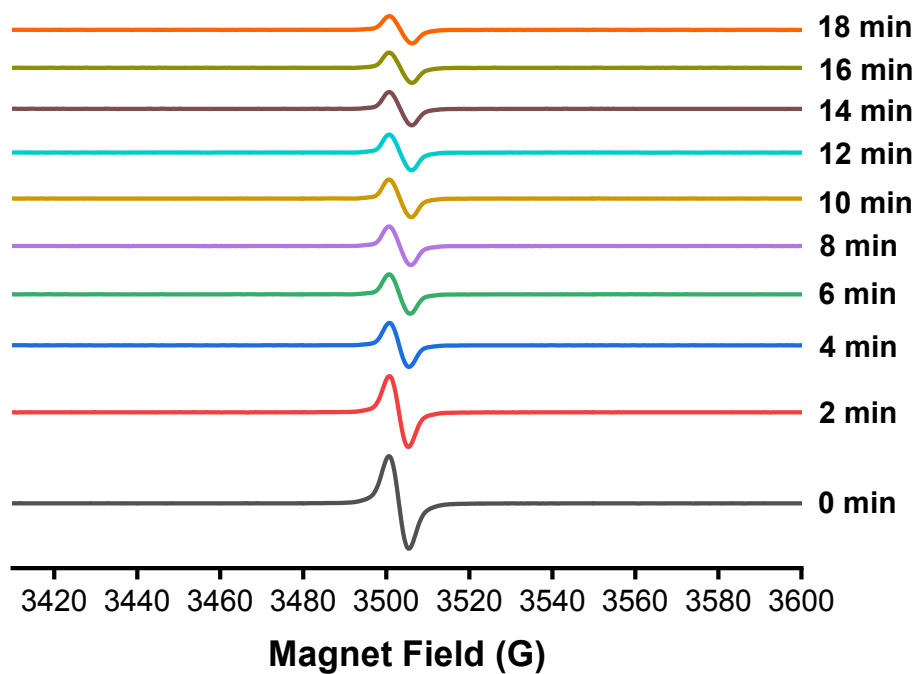


Figure S6. EPR signal fading of M1 (1 mM in N, N-dimethylformamide) upon irradiation at 298 K.

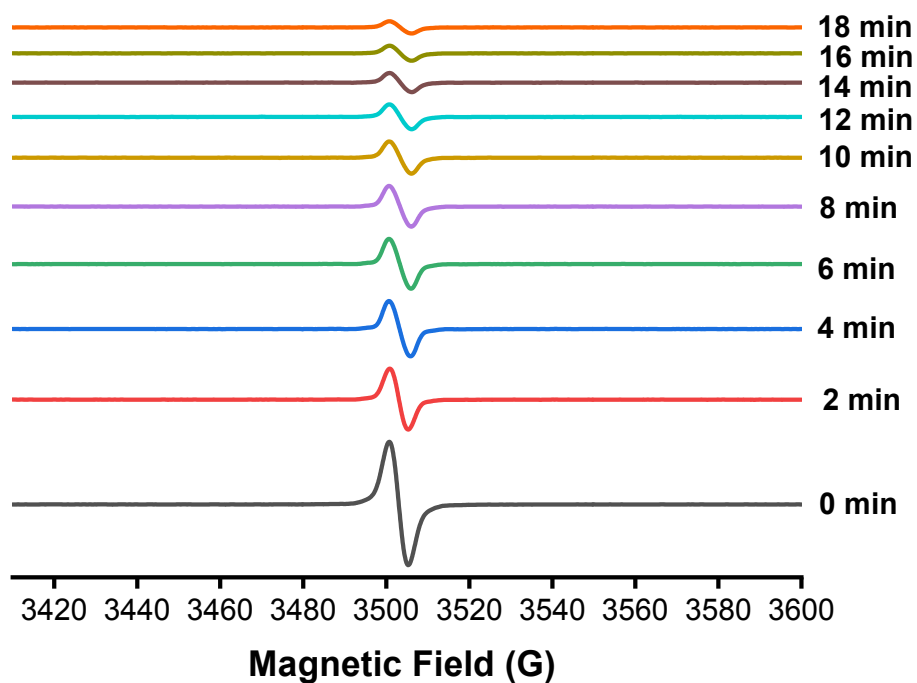


Figure S7. EPR signal fading of **M2** (1 mM in N, N-dimethylformamide) upon irradiation at 298 K.

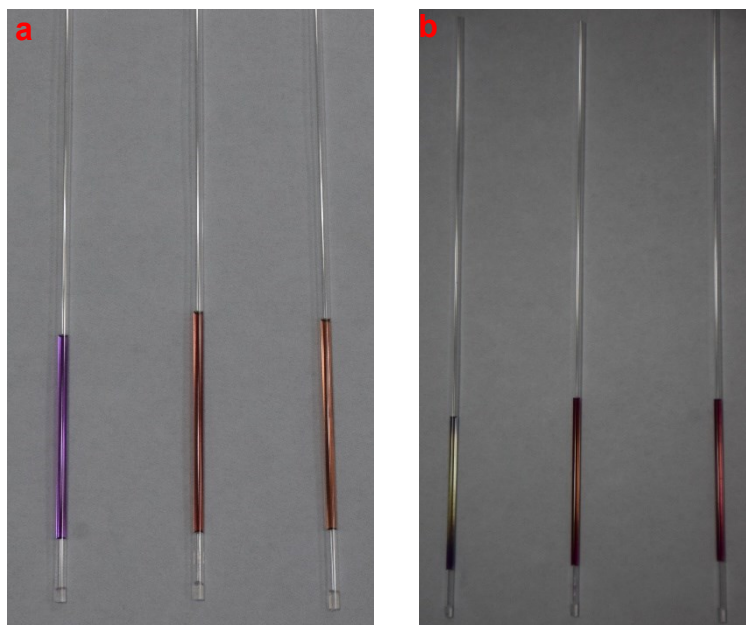


Figure S8. Image of **CzBTM-Py**, **M1** and **M2** (1 mM in N, N-dimethylformamide) before (a) and after (b) irradiation.

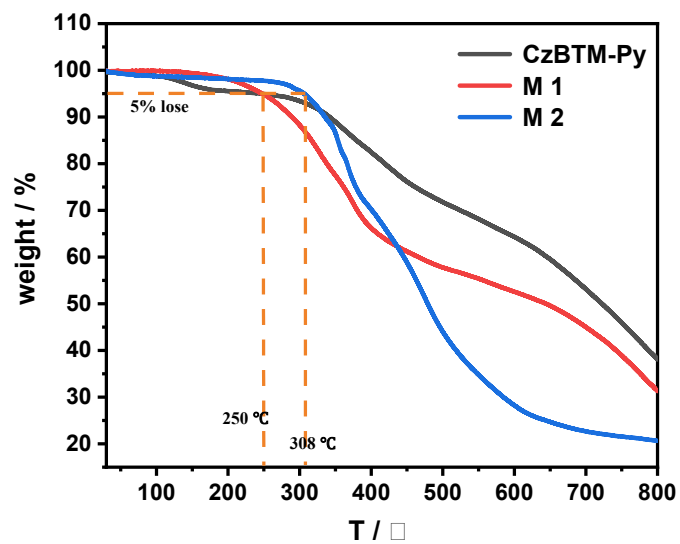


Figure S9. Thermogravimetric analysis of **CzBTM-Py**, **M1** and **M2**.

4 Single crystal data

Table S1. X-ray single crystal data of CzBTM-Py, M1 and M2.

Compound	CzBTM-Py
Empirical formula	C ₃₆ H ₁₉ Cl ₉ N ₃
Formula weight	693.25
Temperature / K	293(2)
Crystal system	monoclinic
Space group	P-1
a / Å	11.0419(4)
b / Å	11.4394(5)
c / Å	14.7194(4)
α / °	81.322(3)
β / °	89.175(2)
γ / °	73.205(3)
Volume / Å ³	1758.73(11)
Z	2
ρ_{calc} / cm ³	1.534
μ / mm ⁻¹	6.815
F (000)	818.0
Crystal size / mm ³	0.48 × 0.36 × 0.24
Radiation	CuK α (λ = 1.54184)
2 θ range for data collection / °	8.17 to 155.876
Index ranges	-13 ≤ h ≤ 13, -14 ≤ k ≤ 14, -18 ≤ l ≤ 18
Reflections collected	37644 7013
Independent reflections	R _{int} = 0.1990, R _{sigma} = 0.0851
Data / restraints / parameters	7013 / 0 / 433
Goodness-of-fit on F ²	1.082
Final R indexes [I ≥ 2 σ (I)]	R ₁ = 0.0854, wR ₂ = 0.2358

Final R indexes [all data]	R ₁ = 0.0934, wR ₂ = 0.2436
Largest diff. peak / hole / e Å ⁻³	1.49 / -1.64
CCDC	2045293

Compound	M1
Empirical formula	C ₁₅₀ H ₁₇₀ Cl ₁₂ F ₂₄ N ₈ P ₁₂ Pt ₄
Formula weight	4118.45
Temperature / K	173(2)
Crystal system	triclinic
Space group	P-1
a / Å	10.0316(3)
b / Å	19.8707(9)
c / Å	27.5647(10)
α / °	108.610(2)
β / °	99.067(2)
γ / °	95.385(2)
Volume / Å ³	5080.9(3)
Z	1
ρ _{calc} / cm ³	1.344
μ / mm ⁻¹	7.911
F (000)	2032.0
Crystal size / mm ³	0.10 × 0.10 × 0.10
Radiation	CuKα (λ = 1.54178)
2θ range for data collection / °	4.748 to 121.132
Index ranges	-11 ≤ h ≤ 11, -20 ≤ k ≤ 22, -31 ≤ l ≤ 31
Data / restraints / parameters	14874 / 1929 / 910
Goodness-of-fit on F ²	1.002
Final R indexes [I ≥ 2σ (I)]	R ₁ = 0.1230, wR ₂ = 0.2838
Final R indexes [all data]	R ₁ = 0.2183, wR ₂ = 0.3332
CCDC	2045295

Compound	M2
Empirical formula	C ₉₆ H ₉₆ Cl ₁₂ F ₆ N ₆ O ₆ P ₄ Pt ₂ S ₂
Formula weight	2845.56
Temperature / K	100.01(11)
Crystal system	monoclinic
Space group	12 / a
a / Å	21.627(2)
b / Å	16.869(2)
c / Å	36.647(4)
α / °	90
β / °	91.494(11)
γ / °	90
Volume / Å ³	13365(3)
Z	4
ρ _{calc} / cm ³	1.266
μ / mm ⁻¹	7.233
F (000)	5072.0
Crystal size / mm ³	0.26 × 0.14 × 0.12
Radiation	CuKα (λ = 1.54184)
2θ range for data collection / °	6.646 to 134.156
Index ranges	-25 ≤ h ≤ 25, -16 ≤ k ≤ 20, -43 ≤ l ≤ 43
Reflections collected	62932 11810
Independent reflections	R _{int} = 0.1930, R _{sigma} = 0.1420
Data / restraints / parameters	11810 / 398 / 574
Goodness-of-fit on F ²	1.288
Final R indexes [I ≥ 2σ (I)]	R ₁ = 0.1501, wR ₂ = 0.3485
Final R indexes [all data]	R ₁ = 0.2292, wR ₂ = 0.3885
Largest diff. peak / hole / e Å ⁻³	2.66 / -1.77
CCDC	2045294

5 NMR spectra of new compounds

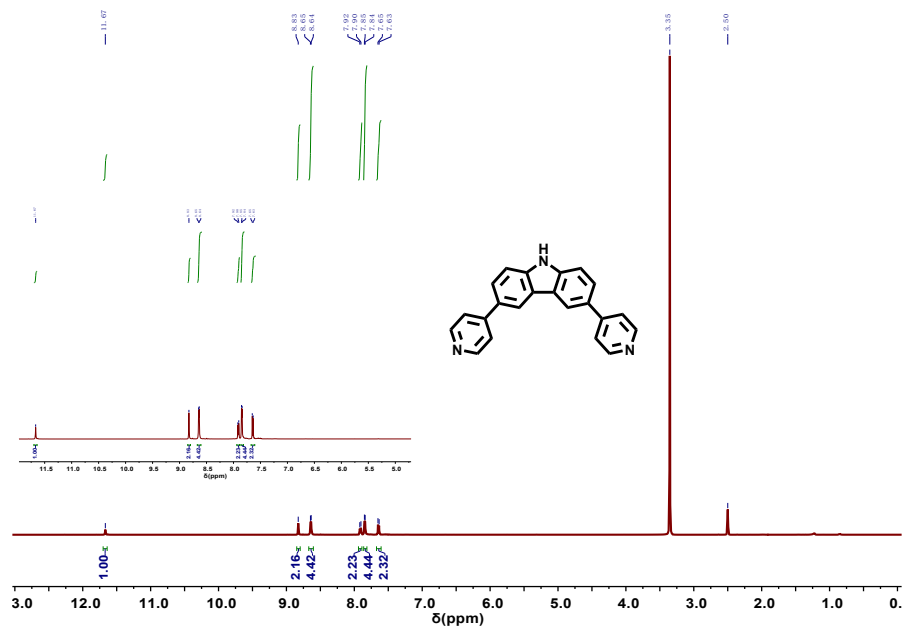


Figure S10. The ¹H NMR (500 MHz, 298 K) spectrum of compound **3** in DMSO-*d*₆.

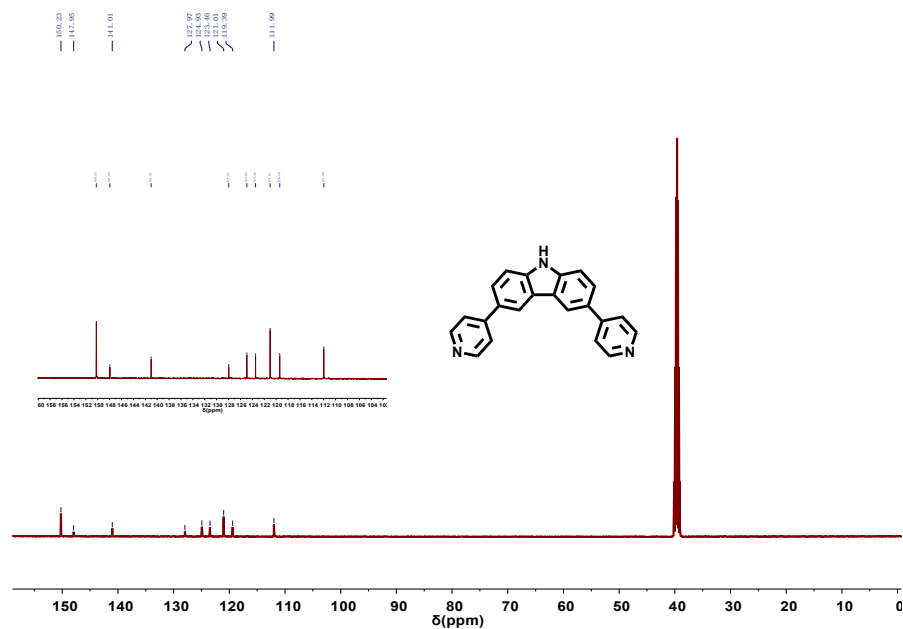


Figure S11. The ¹³C NMR (126 MHz, 298 K) spectrum of compound **3** in DMSO-*d*₆.

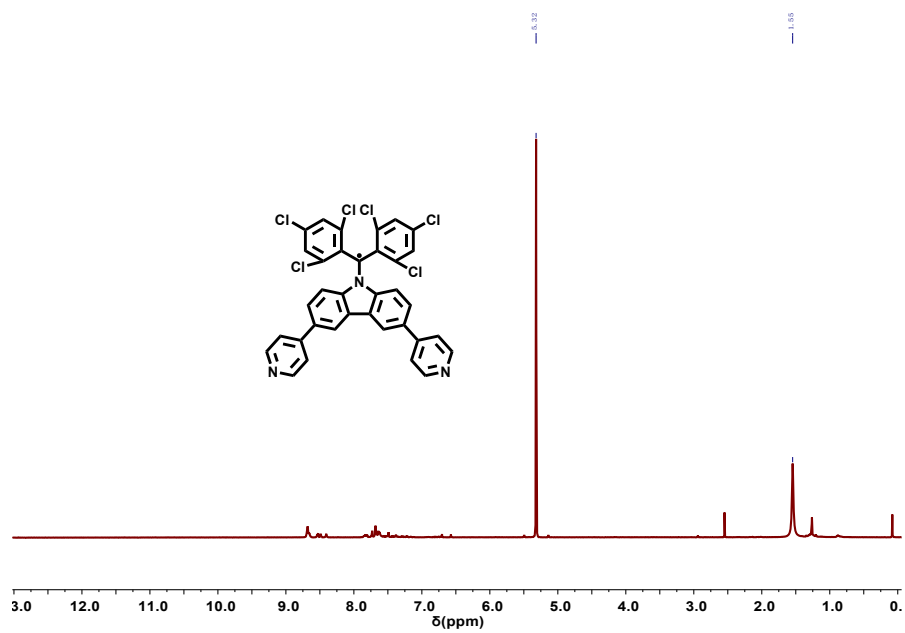


Figure S12. The ¹H NMR (500 MHz, 298 K) spectrum of CzBTM-Py in CD₂Cl₂.

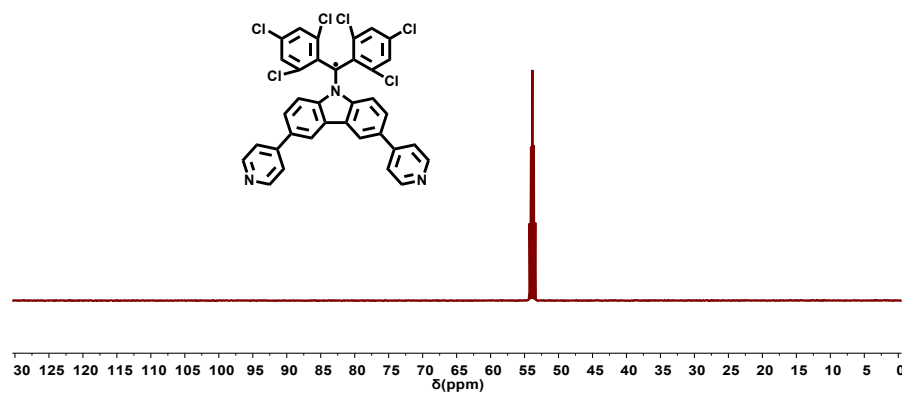


Figure S13. The ¹³C NMR (126 MHz, 298 K) spectrum of compound CzBTM-Py in CD₂Cl₂.

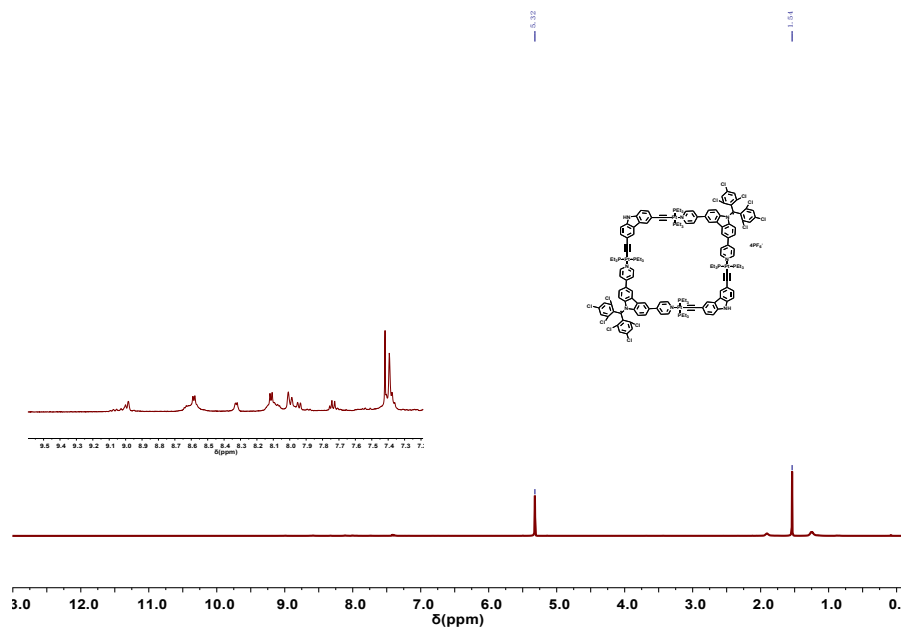


Figure S14. The ^1H NMR (500 MHz, 298 K) spectrum of **M1** in CD_2Cl_2 .

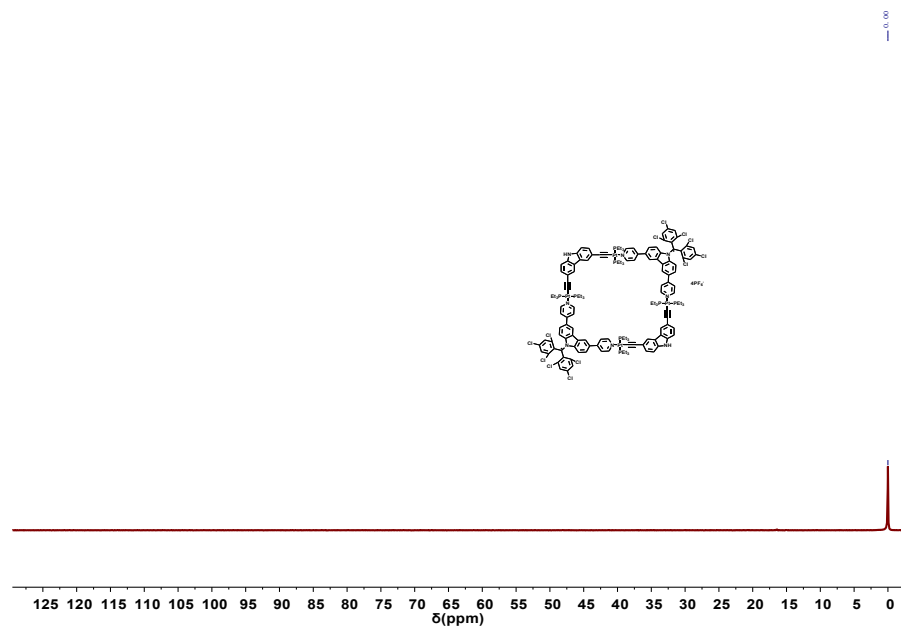


Figure S15. The ^{31}P NMR (202 MHz, 298 K) spectrum of **M1** in CD_2Cl_2 .

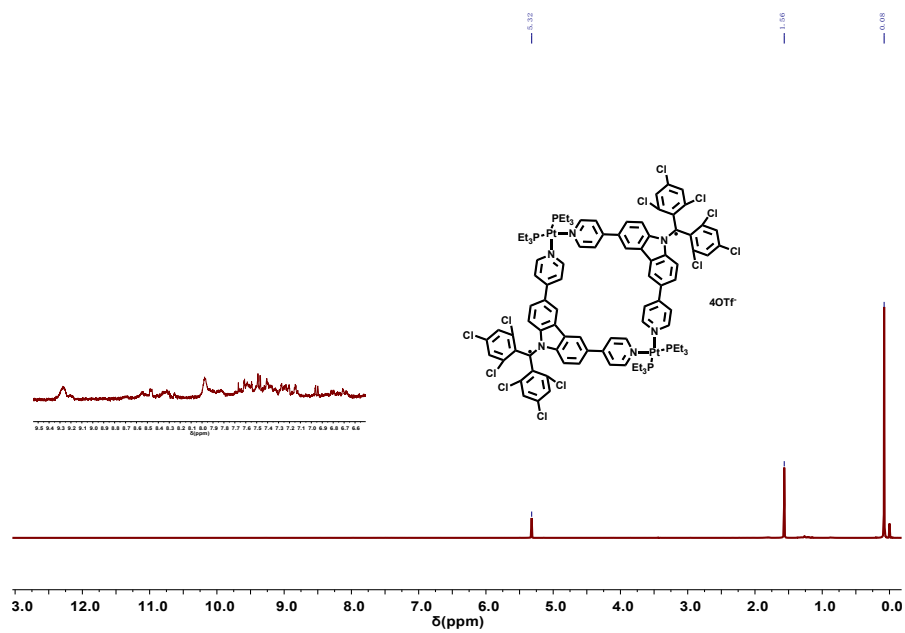


Figure S16. The ^1H NMR (500 MHz, 298 K) spectrum of **M2** in CD_2Cl_2 .

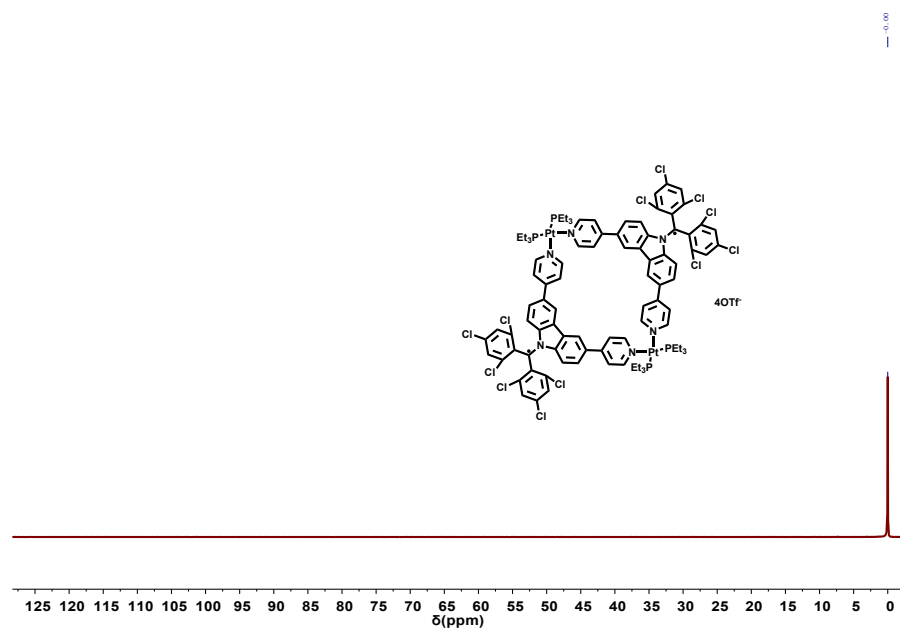


Figure S17. The ^{31}P NMR (202 MHz, 298 K) spectrum of **M2** in CD_2Cl_2 .

6 Mass spectra of new compounds

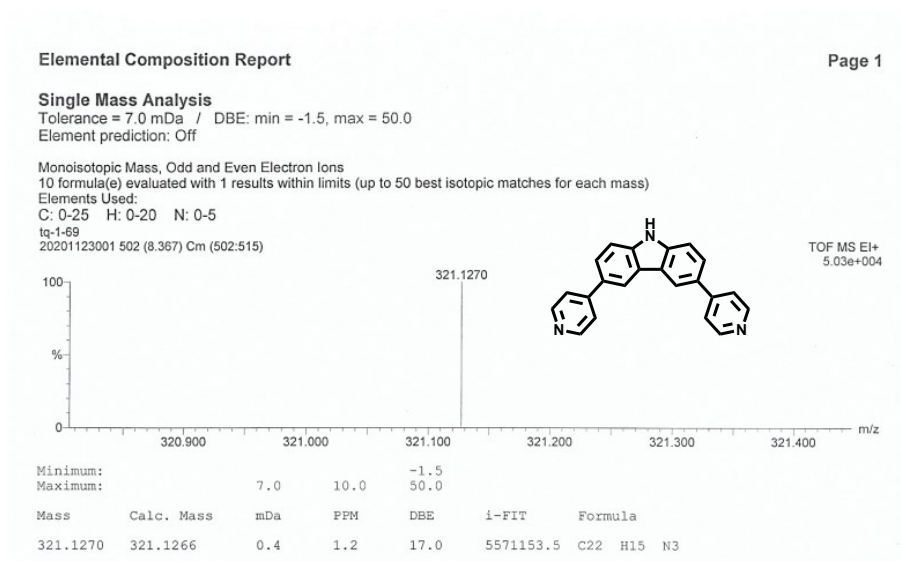


Figure S18. The mass spectrum of compound **3**.

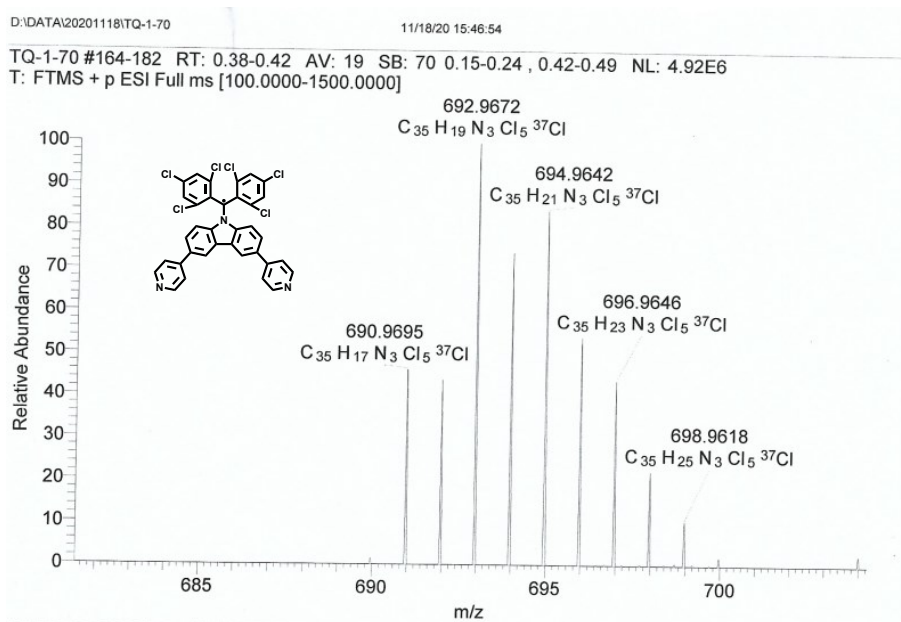


Figure S19. The mass spectrum of compound **CzBTM-Py**.

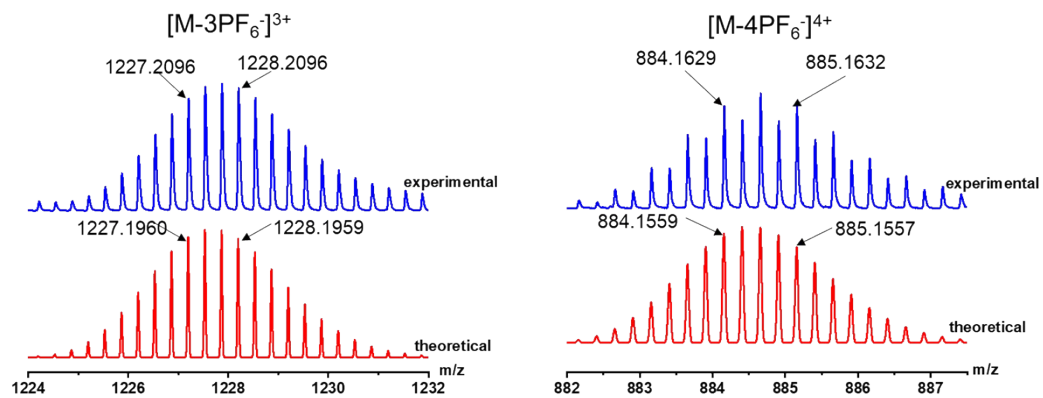


Figure S20. The mass spectrum of compound M1.

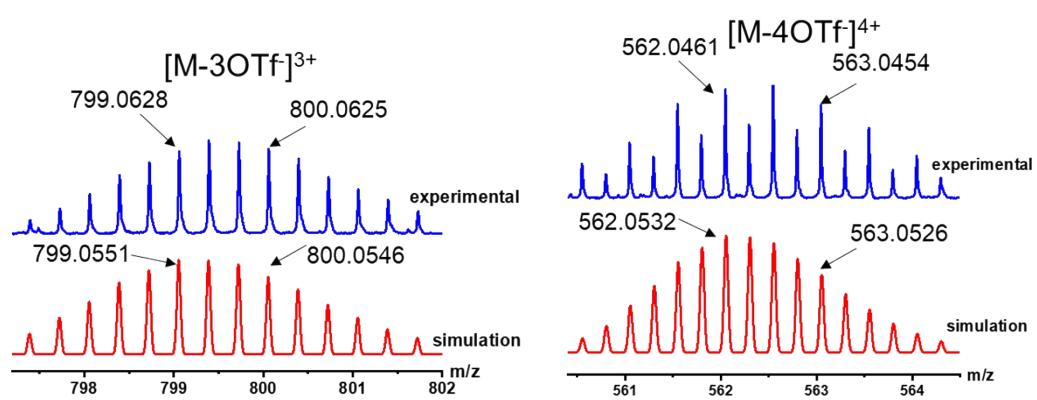


Figure S21. The mass spectrum of compound M2.

7 Photophysical properties

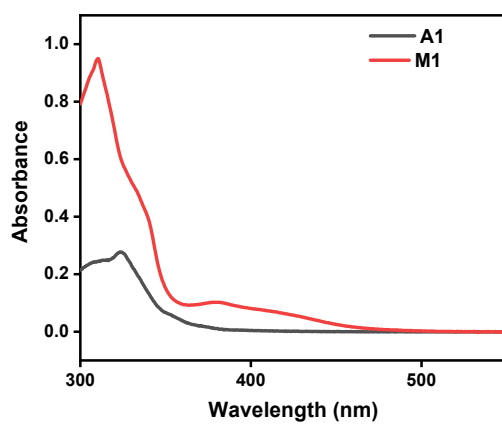


Figure S22. UV-Vis absorption spectra of A1 and M1 (10 μM).

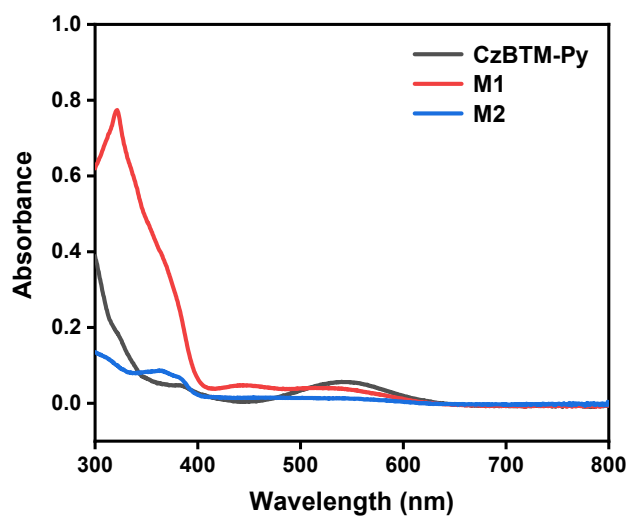


Figure S23. UV-Vis absorption spectra of **CzBTM-Py** ($10 \mu\text{M}$), **M1** and **M2** ($5 \mu\text{M}$).

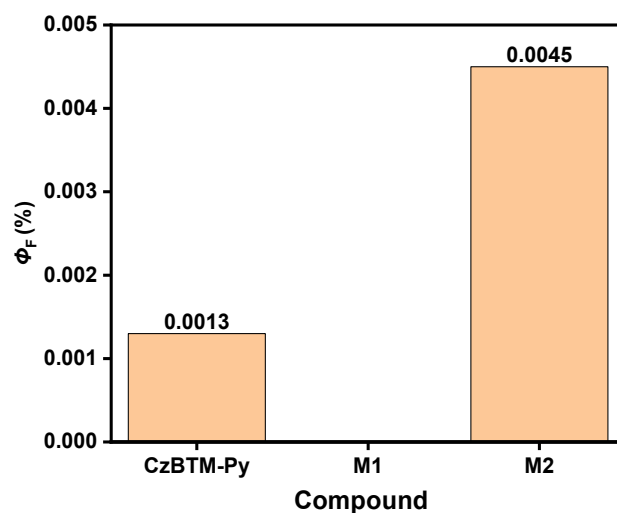


Figure S24. The fluorescence quantum yield of **CzBTM-Py**, **M1** and **M2** ($100 \mu\text{M}$ in dichloromethane).

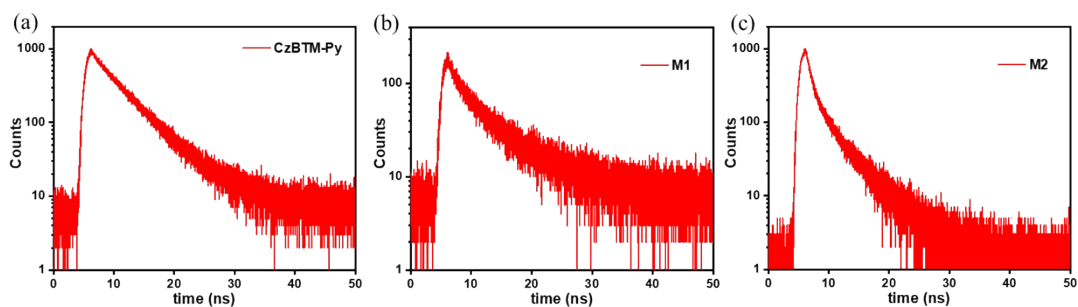


Figure S25. Time-resolved fluorescence decay curves ($100 \mu\text{M}$, 400 nm excitation and 450 nm detection). (a) **CzBTM-Py**; (b) **M1**; (c) **M2**.

Table S2. The fluorescence lifetimes of **CzBTM-Py**, **M1** and **M2** (100 μM in dichloromethane, 400 nm excitation and 450 nm detection).

Compound	τ_1 (ns)	τ_2 (ns)
CzBTM-Py	1.36 (81.4%)	4.99 (18.6%)
M1	1.62 (95.4%)	7.48 (4.6%)
M2	4.43 (99.9%)	0.85 (0.1%)

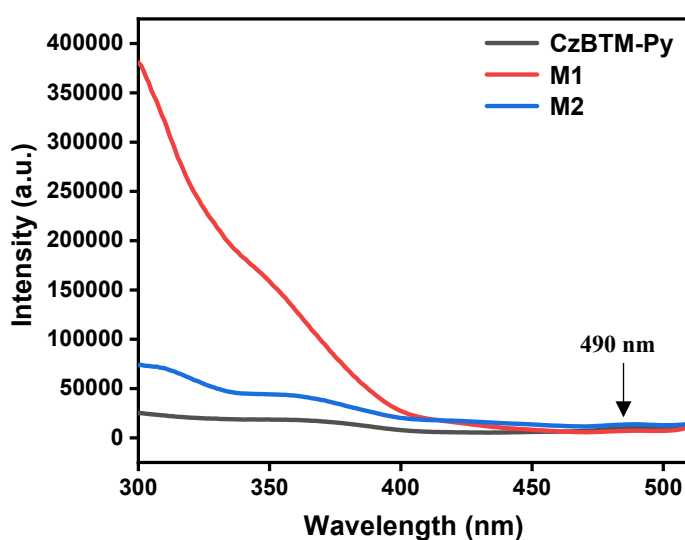


Figure S26. The excitation spectrum of **CzBTM-Py** (10 μM , $\lambda_{\text{em}} = 534.5$ nm), **M1** and **M2** (5 μM in dichloromethane, $(\lambda_{\text{em}})_{\text{M1}} = 551$ nm, $(\lambda_{\text{em}})_{\text{M2}} = 552$ nm, slit widths: 20 nm/20 nm).

8 Theoretical calculations results

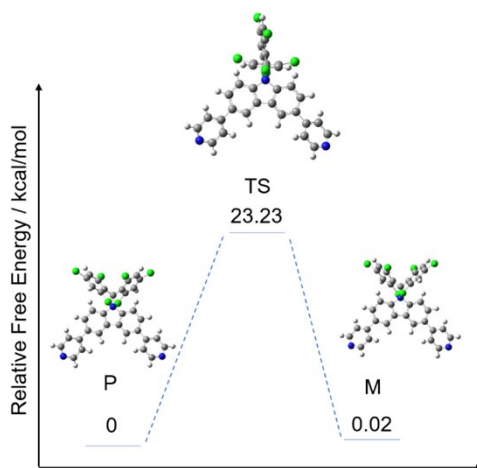


Figure S27. Energy diagram of the racemization process of **CzBTM-Py**.

Table S3. Energy barrier calculation details of **CzBTM-Py**.

	P	M	TS
Thermal Correction to Free Energy / Hartree	0.361506	0.361506	0.362256
Electronic energy / Hartree	-4269.552364	-4269.552331	-4269.516099
Gibbs Free Energy / Hartree	-4269.190858	-4269.190825	-4269.153843
Relative Free Energy / kcal/mol	0	0.02	23.23

Computational details:

1. The geometries were optimized at UB3LYP^{4,5}-D3(BJ)⁶/6-31G* level and harmonic frequency calculations were performed at the same level by Gaussian 16⁷.
2. Gibbs Free energy (gas phase, 298.15 K, 1 atm) = Electronic energy + Thermal Correction to Free Energy.
3. Electronic energy is calculated at the RI-PWPB95⁸/def2-QZVPP level by ORCA 4.2⁹.

9 Reference

- [1] X. Ai, Y. X. Chen, Y. T. Feng and F. Li, A Stable Room-Temperature Luminescent Biphenylmethyl Radical, *Angew. Chem. Int. Ed.*, **2018**, 57,2869-2873.
- [2] S. Shanmugaraju, A. K. Bar, K.-W. Chi and P. S. Mukherjee, Coordination-Driven Self-Assembly of Metallamacrocycles via a New Pt^{II}₂ Organometallic Building Block with 90° Geometry and Optical Sensing of Anions, *Organometallics*, **2010**, 29, 2971-2980.
- [3] F. Fochi, P. Jacopozzi, E. Wegelius, K. Rissanen, P. Cozzini, E. Marastoni, E. Fiscaro, P. Manini, R. Fokkens and E. Dalcanale. Self-Assembly and Anion Encapsulation Properties of Cavitand-Based Coordination Cages. *J. Am. Chem. Soc.*, **2001**, 123, 7539-7552.
- [4] A. D. Becke, Density-functional thermochemistry. III. The role of exact exchange, *The Journal of Chemical Physics*, **1993**, 98, 5648-5652.
- [5] C. Lee, W. Yang and R. G. Parr, Development of the Colle-Salvetti correlation-energy formula into a functional of the electron density, *Physical review B*, **1988**, 37, 785.
- [6] S. Grimme, S. Ehrlich and L. Goerigk, Effect of the damping function in dispersion corrected density functional theory, *Journal of Computational Chemistry*, **2011**, 32, 1456-1465.
- [7] M. Frisch, G. Trucks, H. Schlegel, G. Scuseria, M. Robb, J. Cheeseman, G. Scalmani, V. Barone, G. Petersson and H. Nakatsuji, Gaussian 16, Revision A. 03, Gaussian Inc., Wallingford CT 2016.
- [8] L. Goerigk and S. J. Grimme, Efficient and Accurate Double-Hybrid-Meta-GGA Density

Functionals—Evaluation with the Extended GMTKN30 Database for General Main Group Thermochemistry, Kinetics, and Noncovalent Interactions, *Chem. Theory Comput.*, **2011**, *7*, 291–309.

[9] F. Neese, F. Wennmohs, U. Becker and C. Riplinger, The ORCA quantum chemistry program package, *J. Chem. Phys.*, **2020**, *152*, 224108.